The Pharma Innovation Journal 2022; SP-11(8): 1088-1102

www.ThePharmaJournal.com

The Pharma Innovation

ISSN (E): 2277-7695
ISSN (P): 2349-8242
NAAS Rating: 5.23
TPI 2022; SP-11(8): 1088-1102

www.thepharmajournal.com
Received: 14-05-2022
Accepted: 26-07-2022

A Eswari
Department of PS&IT, AEC&RI, TNAU, Coimbatore, Tamil Nadu, India

A Subbiah
Grape Research Station, Theni, Tamil Nadu, India

MR Duraisamy
Department of PS&IT, AEC&RI, TNAU, Coimbatore, Tamil Nadu, India

K Manonmani
Department of Pl. Pathology, AC&RI, TNAU, Madurai, Tamil Nadu, India

Corresponding Author
A Eswari
Department of PS&IT, AEC&RI, TNAU, Coimbatore, Tamil Nadu, India

A generic yield prediction model for grapes under agro climatic conditions based on disease management

A Eswari, A Subbiah, MR Duraisamy and K Manonmani

DOI: https://doi.org/10.22271/tpi.2022.v11.i8Sn.14909

Abstract
Climate has a direct influence on crop development and the final yield. In this article, a generic agro climatic yield prediction model for grape is developed and analytically solved. This model is useful for research scholars, faculty members and academicians in the area of mathematical biology. The asymptotic analysis is carried out to obtain the final form of the yield prediction model. In the process of model development, climate, disease and grape yield are considered as dependent parameter. Infection rate, disease incidence, seasonality rate and removal rate of grape yield per harvest time are considered as independent parameters. Further, the model is studied and the parameters estimation from the field level data during the period 2015-2021 from GRS and Theni surrounding villages. The effects of various parameters on concentration curves are discussed. Stability Analysis of this model is also explained. The obtained analytical solution in comparison with the numerical and stability analysis is found to be in satisfactory agreement. In addition, the basic reproduction number for this model is obtained. This model helps to predict the future calculations of infected and recovered yield for grape from the reproduction number R_0. The model permits to highlight crucial mechanisms to undergo and evaluate the consequences of different agricultural practices on the quantity and quality of the yield.

Keywords: Seasonality rate, grape yield, disease incidence, infection rate, mathematical modeling, simulation

1. Introduction
Climate has a profound influence on vine growth, productivity and quality of fruits. Of the factors contributing to the successful cultivation of grape, climate ranks first. The weather parameters *viz*., sun light, rainfall, humidity also influence the quality development of the fruits.

Downy Mildew (*Plasmopara viticola*) is known as one of the most important vineyard diseases in TamilNadu, because it has the capability to develop and spread very quickly and cause large crop losses in certain areas according to the weather conditions [1]. Farmers must make decisions whether or not to spray downy mildew and also how frequently to spray and which agrochemicals to use [2]. A good understanding of the stage is needed in incidence and conditions of congenial for the incidence and development of the disease. The efficacy and mode of action of fungicides help the effective management of any disease, particularly downy mildew.

Some mathematical models are developed to provide short-term and field-scale predictions of DM epidemics resulting from infections caused by P. Viticola sporangia in Switzerland, France, Austria, Germany, and Italy [3-10]. These models are developed by using a common database of previous publications.

Christopher *et al*. have reformulated the SIR model with host response to infection load for a plant disease [11]. Daniele *et al*. [12] have developed the model for temporal dynamics of brown rot spreading in fruit orchards. Jeger *et al*. [13] have developed a generic modelling framework to understand the dynamics of foliar pathogen and bio-control agent (BCA) populations in order to predict the likelihood of successful bio-control in relation to the mechanisms involved. Abdul Latif has formulated the induced resistance to plant disease using a dynamical system approach [14]. Mario de la fuente has compared different methods of grapevine yield prediction in the time window between fruit set and version [15]. Rory Ellis *et al*. [16] have developed the Bayesian growth model to predict the yield for grape by using simulation. A dynamic model for *Plasmopara viticola* primary infections on grapevine was elaborated according to a mechanistic approach by Vittorio Rossi [17]. A generic mathematical model that incorporates the elicitor effect to combat disease infection was initially introduced by Abdul

Latif [18]. Manisha S. Sirsat [19] obtained the predictive model for each phenology that predicts yield during growing stages of grapevine and to identify highly relevant predictive variable by machine learning technique. Recently, a prediction model has been developed for the Godello cultivar, one of the preferential autochthonous white cultivars in the Northwest Spain Ribeiro Designation of Origin vineyards, by means of aerobiological, meteorological and flower production analysis by Estefanía González-Fernández [20]. More recently, Kadbhane *et al*. [21] have developed the grape yield (ACGY) model under climate change scenario using multiple linear regression analysis.

According to the literature survey, there are many yield estimating models that can be used to estimate the yield of wheat, rice, maize, sorghum, sugarcane, etc. However, for grapes, there are no models available for estimation without secondary data. So far, no models have been reported for estimation exactly of grape yield in Indian terrain. The present study aims at developing an agro-climatic grape yield prediction model for the study area in Theni district based on current and future climate data. However, to the best of our knowledge, till date no general model and analytical results for the concentration of climate, disease and yield of grape as a function of infection rate, disease incidence, seasonality rate and removal rate of grape yield loss per harvest time**.** The obtained analytical solution in comparison with the numerical and stability analysis is found to be in satisfactory agreement. In addition, the basic reproduction number for yield prediction model for grape is obtained.

2. Mathematical formulation of the problem

In the development of the yield prediction model, temperature, relative humidity, rainfall, and rainy days etc., are all considered climate domain characteristics. Climate data is collected by a groundnut centre in Tamil Nadu. Field surveys are used to obtain data on the incidence domain, while the Grape research station in Theni collected yield data during the period 2015-2021.All grape plants are of common variety cultivated in the study area, namely Muscat Humbug. Figure 1 shows the agro-climatic disease grape yield model schematic diagram used for real-life theoretical outcome.

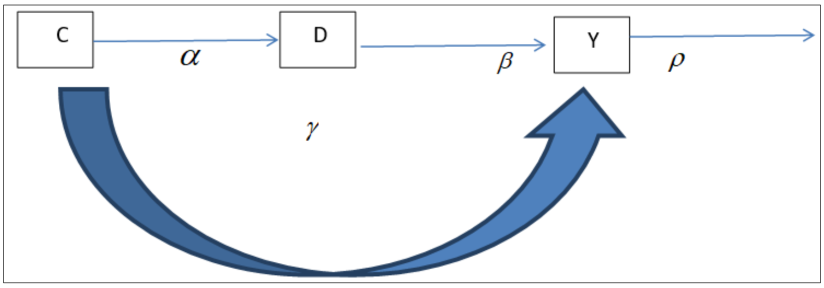

Fig 1: The agro-climatic disease grape yield model schematic diagram used for real-life theoretical outcome

The parameters from the domain γ is the seasonality rate, β is the disease incidence, α is the infection rate and ρ is the removal rate of yield loss per harvest time. It is considered in the development of the agro-climatic grape yield prediction model using the asymptotic analysis. The basic form of the model is indicated below:

$$\frac{dC}{dt} = -\alpha CD - \gamma C \tag{1}$$

$$\frac{dD}{dt} = \alpha CD - \beta D \tag{2}$$

$$\frac{dY}{dt} = \beta D + \gamma C - \rho Y \tag{3}$$

The corresponding initial conditions are:

$$C(0) = C^*; D(0) = D^*, Y(0) = Y^* \tag{4}$$

where C is the concentration of climate, D is the concentration of disease, Y is the concentration of yield, t is the time in days, α is the infection rate for grape, β is the disease incidence rate for grape, γ is the seasonality rate, ρ is the removal rate of grape yield loss per harvest time, using HPM (Appendix A) to find the solution of the equations (1-3) is

$$C(t) = C^* e^{-\gamma t} - \frac{\alpha C^* D^*}{\beta} e^{-\gamma t} + \frac{\alpha C^* D^*}{\beta} e^{-(\beta+\gamma)t} + \left(\frac{\alpha^2 C^{*2} D^*}{\beta\gamma} - \frac{\alpha^2 C^{*2} D^*}{(\beta+\gamma)} - \frac{\alpha^2 C^* D^{*2}}{2\beta^2} \right) e^{-\gamma t} - \frac{\alpha^2 C^{*2} D^*}{\beta\gamma} e^{-(\beta+\gamma)t}$$
$$+ \frac{\alpha^2 C^{*2} D^*}{(\beta+\gamma)} e^{-(\beta+2\gamma)t} + \frac{\alpha^2 C^* D^{*2}}{\beta^2} e^{-(\beta+\gamma)t} - \frac{\alpha^2 C^* D^{*2}}{2\beta^2} e^{-(2\beta+\gamma)t} \tag{5}$$

$$D(t)=D^{*}e^{-\beta t}+\frac{\alpha C^{*}D^{*}}{\gamma}e^{-\beta t}-\frac{\alpha C^{*}D^{*}}{\gamma}e^{-(\beta+\gamma)t}+\left(\frac{\alpha^{2}C^{*2}D^{*}}{2\gamma^{2}}-\frac{\alpha^{2}C^{*}D^{*2}}{\gamma\beta}+\frac{\alpha^{2}C^{*}D^{*2}}{(\beta+\gamma)}\right)e^{-\beta t}$$
$$-\frac{\alpha^{2}C^{*2}D^{*}}{\gamma^{2}}e^{-(\beta+\gamma)t}+\frac{\alpha^{2}C^{*2}D^{*}}{2\gamma^{2}}e^{-(\beta+2\gamma)t}+\frac{\alpha^{2}C^{*}D^{*2}}{\gamma\beta}e^{-(\beta+\gamma)t}-\frac{\alpha^{2}C^{*}D^{*2}}{(\beta+\gamma)}e^{-(2\beta+\gamma)t} \quad (6)$$

$$Y=Y^{*}e^{-\rho t}+\left(\frac{\gamma C^{*}}{\gamma-\rho}+\frac{\beta D^{*}}{\beta-\rho}\right)e^{-\rho t}+\frac{\gamma C^{*}}{\rho-\gamma}e^{-\gamma t}+\frac{\beta D^{*}}{\rho-\beta}e^{-\beta t} \quad (7)$$

3. Local stability analysis
3.1 Equilibria
An equilibrium point is a point at which variables of a system remain unchanged over time. An equation (1)-(3) possesses the equilibrium $\left(\frac{\beta}{\alpha},0,\frac{\beta\gamma}{\alpha\rho}\right)$ and the system is stable at this equilibrium point. If the system is at stable steady state and is perturbed slightly off the steady state, then the system will return to the steady state. Therefore, small fluctuations in crops will not destroy the equilibrium and it would expect to observe such equilibrium in nature. In this way, the stability typically determines physically viable behavior. It is now determined that the behaviour of equations (1)-(3) near the equilibrium point find the linearization at the equilibrium. Jacobian matrix is needed to assess.

$$J=\begin{pmatrix}-\alpha D-\gamma & -\alpha C & 0\\ \alpha D & \alpha C-\beta & 0\\ \gamma & \beta & -\rho\end{pmatrix}$$

At an equlibrium point

$$J=\begin{pmatrix}-\gamma & -\beta & 0\\ 0 & 0 & 0\\ \gamma & \beta & -\rho\end{pmatrix}$$

Eigen values of the Jacobian matrix are $\lambda_1=0,\lambda_2=-\rho,\lambda_3=-\gamma.$

In our system, $\mathrm{Re}(\lambda_i)\le 0$,so the given system is stable. It is clear to see that the system (1)-(3) has disease-free equilibrium $\left(\frac{\beta}{\alpha},0,\frac{\beta\gamma}{\alpha\rho}\right)$. Let $X=(C,D,Y)^{T}$, then the system (1)-(3) can be written as $X^{'}=F(X)-V(X).$

where,

$$F(X)=\begin{bmatrix}0\\ \alpha CD\\ \beta D\end{bmatrix} \text{and} V(X)=\begin{bmatrix}\alpha CD+\gamma C\\ \beta D\\ -\gamma C+\rho Y\end{bmatrix}$$

The Jacobian matrices of $F(X)$ and $V(X)$ at the disease free equilibrium points are respectively. Let,

$$F=\langle J(F(X))\rangle_{\left(\frac{\beta}{\alpha},0,\frac{\beta\gamma}{\alpha\rho}\right)}=\begin{bmatrix}0 & 0 & 0\\ 0 & \beta & 0\\ 0 & \beta & 0\end{bmatrix}, \quad V=\langle J(V(X))\rangle_{\left(\frac{\beta}{\alpha},0,\frac{\beta\gamma}{\alpha\rho}\right)}=\begin{bmatrix}\gamma & \beta & 0\\ 0 & \beta & 0\\ -\gamma & 0 & \rho\end{bmatrix}$$

Then, $V^{-1} = \frac{1}{\rho\beta\gamma}\begin{bmatrix} \beta\rho & -\beta\rho & 0 \\ 0 & \rho\gamma & 0 \\ \beta\gamma & -\beta\gamma & \beta\gamma \end{bmatrix}$ and $FV^{-1} = \frac{1}{\rho\beta\gamma}\begin{bmatrix} 0 & 0 & 0 \\ 0 & \rho\beta\gamma & 0 \\ 0 & \rho\beta\gamma & 0 \end{bmatrix}$

Stability can be analyzed using direction filed, numerical method in figure 9. Thus, $R_0 = spectrum\ (FV^{-1}) = 1$, the given system is globally stable. It has formulated a yield prediction model and investigated the dynamical behaviors. It has also obtained the basic reproduction number, R_0 which plays a crucial role. By constructing Lyapunov function, it proves the global stability of the equilibria: when the basic reproduction number is less than or equal to one, all solutions converge to the disease-free equilibrium that is disease dies out eventually.

4. Numerical Solution

The model formulation of the equation is numerically solved to test the accuracy of this analytical method. Eqs. (1-3) are numerically solved using Matlab software, a programme that may be used to solve initial value problems. A complete Matlab application for numerical simulation is included in Appendix B. The comparison confirmed that the numerical results match visually and tabular analytical results extremely well. For using field level data during the period 2015-2021(in Tables 2-5), the seasonality rate, the disease incidence, the infection rate and the removal rate of yield loss per harvest time is obtained and applied in the given analytical result. There is no significant difference in error % between the numerical and analytical results.

5. Result and discussion

Eqs. (5-7) are the new analytical expressions of the climate, disease and yield as a function of the seasonality index, the disease incidence, the infection rate and the removal rate of yield loss per harvest time. The concentration of a species is determined by the varying relative rates of infection rate, disease severity as well as effective seasonality rate. The concentration of $C(t), D(t)$ and $Y(t)$ involved in the infection rate, seasonality index and diseases severity with respect to the time in days from the agro-climatic grape yield model and compared with numerical results in Fig. 2. From the figure, it is observed that the concentration of climate is increasing when disease is automatically increasing and other concentration yield becomes zero at initial time. Due to longtime, the concentration of climate is decreasing when disease is automatically decreasing at the same time the concentration of yield is increases. The concentration profile is equal to steady state when time in days ($t \geq 1$). The effects of seasonality index C^* on concentration of climate as a function of time (days) with $D^* = 0, Y^* = 0, \alpha = 23.98, \beta = 24.04, \gamma = 90$ are shown in Fig. 3. As it increases, the concentration of climate decreases. Fig. 4 shows the effects of infection rate α on concentration of disease as a function of time (days) using Eq. 6, where it is observed that the concentration of disease increases when the infection rate increases. Fig. 5 demonstrates quantitatively the effects of seasonality rate parameter on the concentration of yield as a function of time in days. At low time, the effect of decreasing seasonality rate on the concentration yield is shown to reduce the yield concentration.

Fig. 6 shows the three-dimension space on the concentration of climate for varying effective seasonality rate and infection rate. The concentration of climate is independent of both α and γ but is a function of C^* where reduces the concentration of climate. Fig. 7, the concentration of disease varies with infection rate and disease incidence for large value of t. In this regime, the concentration of disease increases with increasing infection rate when $\beta < 10$. In figure 8, the disease incidence β is extremely high, when the concentration of yield asymptotically reaches a constant value regardless of γ, but it depends on α. It can be concluded that the concentration of yield increases, when the seasonality index and disease incidence slightly decrease. Analytical expression of climate, disease and yield are compared with simulation results in Table 1. The maximum relative error between numerical simulations with the analytical result for the developed model is obtained 0.2832%. Stability analysis is carried out for the developed model using the parametric Jacobian transformation method. Based on the obtained results of the mathematical tests, the developed yield prediction model (Eq.5-7) is recommended for its use to estimate the grape yield. Further, phase portraits, for both linear and non linear system can be predicted or analyzed using algebraic method. In figure 9, is easy to see that the globally stable state and the both upper and lower are positive state are stable nodes.

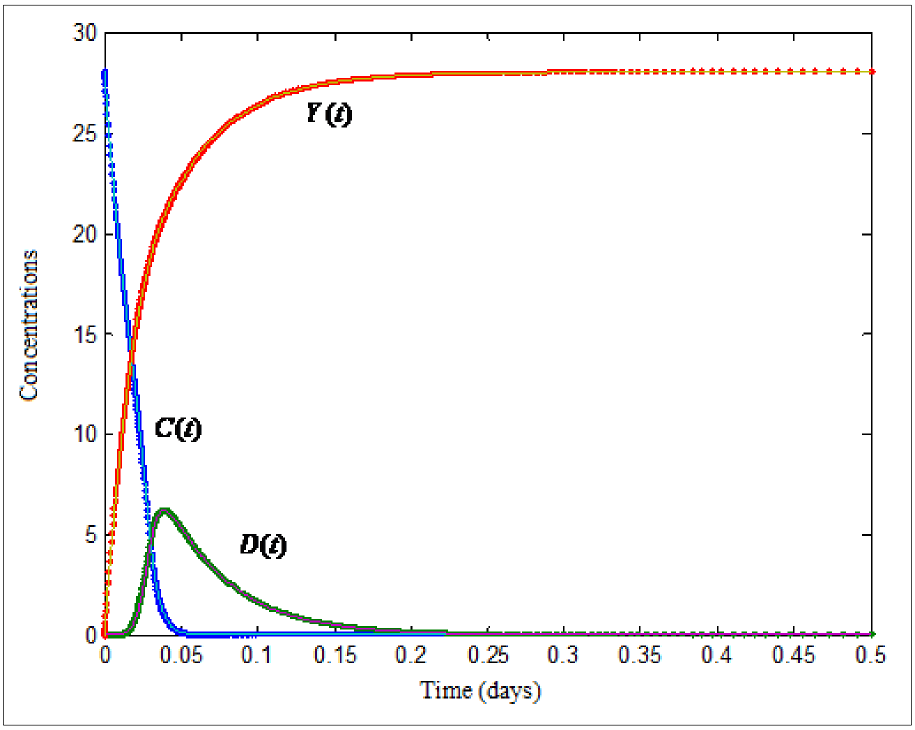

Fig 2: Concentrations for $C(t), D(t)$ and $Y(t)$ versus time in days for $C^* = 33, D^* = 0, Y^* = 0, \alpha = 23.98, \beta = 24.04, \gamma = 90, \rho = 0.2.$ The dotted line represent the numerical results and solid line represents the analytical results.

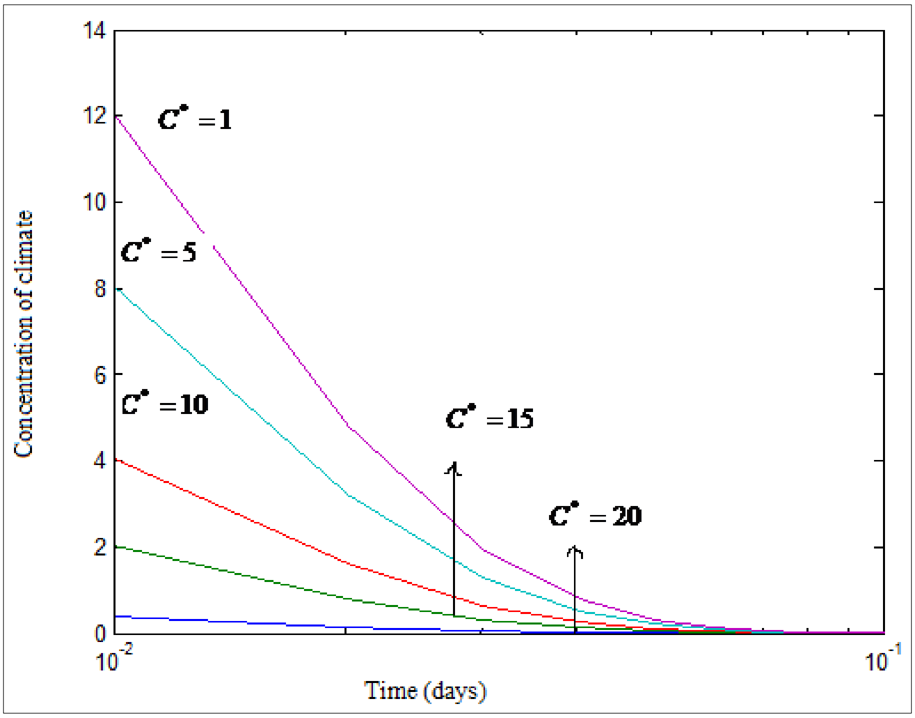

Fig 3: Effects of seasonality index C^* on concentration of climate as a function of time (days) with $D^* = 0, Y^* = 0, \alpha = 23.98, \beta = 24.04, \gamma = 90.$

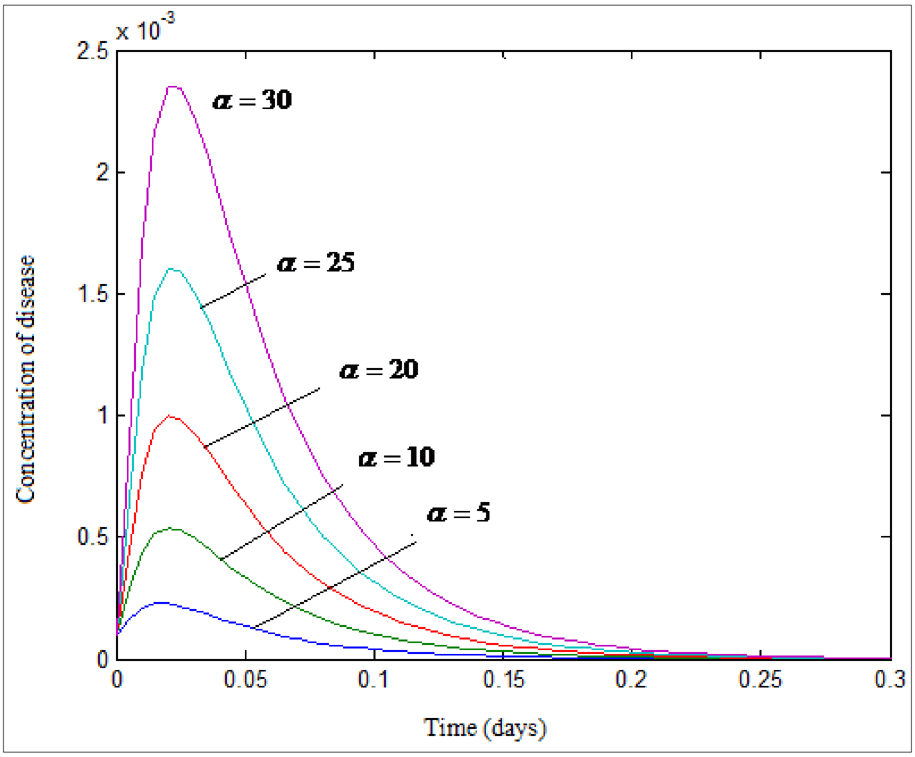

Fig 4: Effects of infection rate α on concentration of disease as a function of time (days) with $C^* = 33, D^* = 0, Y^* = 0, \beta = 24.04, \gamma = 90.$

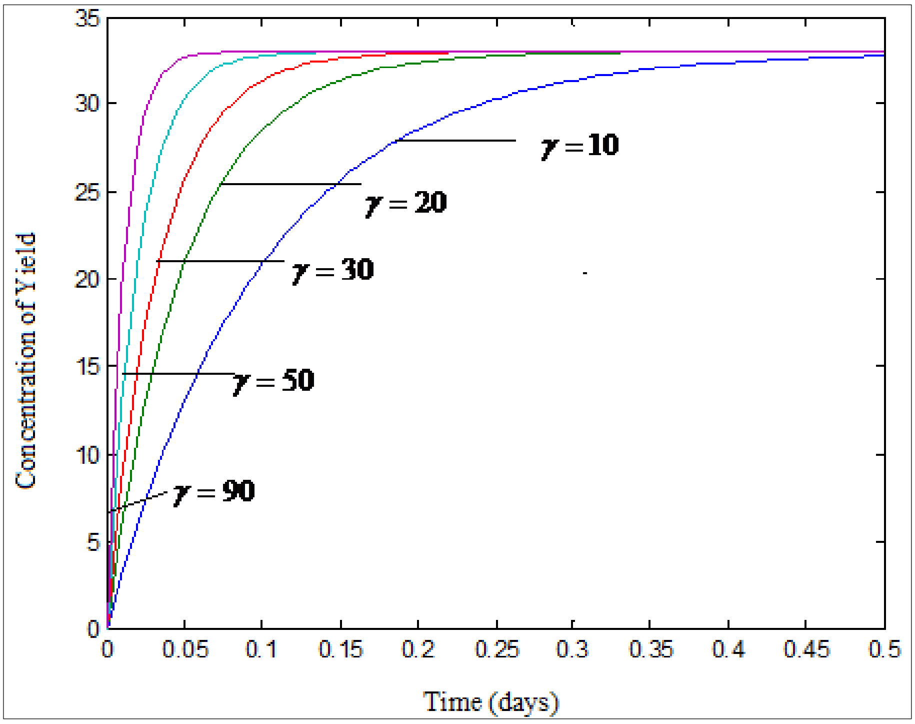

Fig 5: Effects of effective seasonality rate γ on concentration of yield as a function of time (days) with

$$C^* = 33, D^* = 0, Y^* = 0, \alpha = 23.98, \beta = 24.04, \rho = 0.2.$$

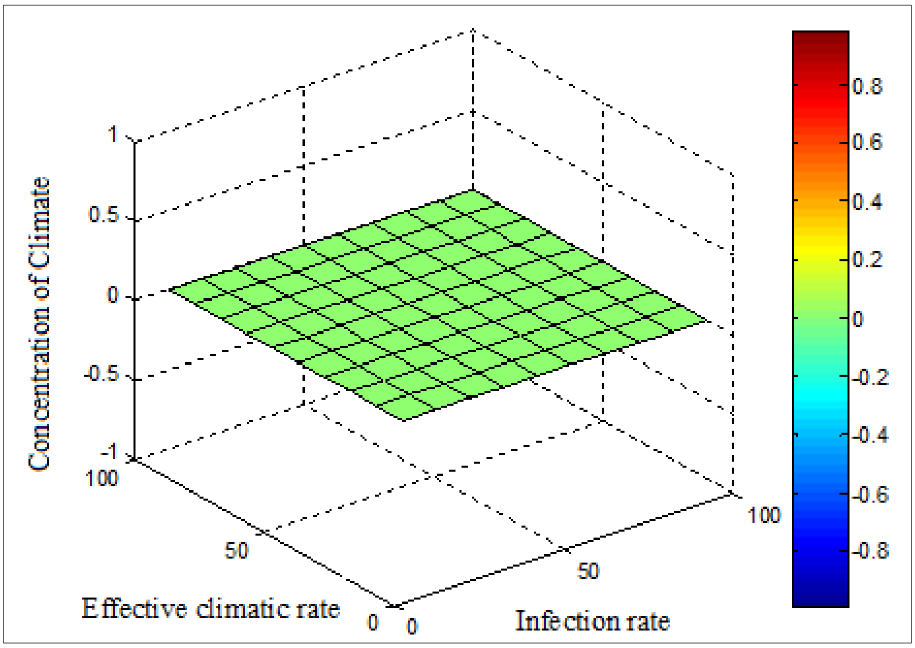

Fig 6: Effects of disease incidence β on concentration of climate for varying effective seasonality rate and infection rate for

$$C^* = 33, D^* = 0, Y^* = 0.$$

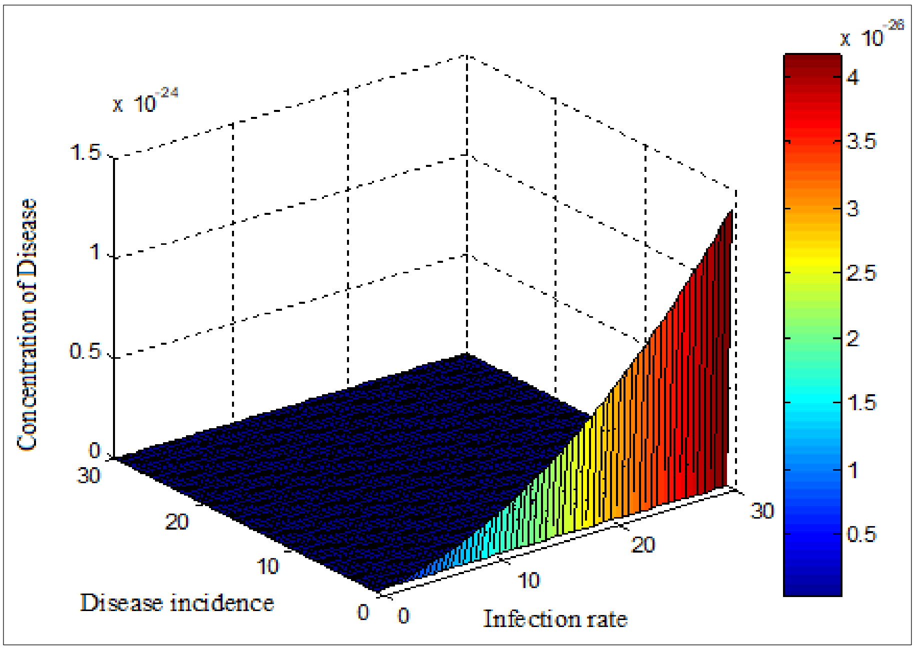

Fig 7: Effects of effective seasonality rate γ on concentration of disease for varying infection rate and disease incidence for

$$C^* = 33, D^* = 0, Y^* = 0.$$

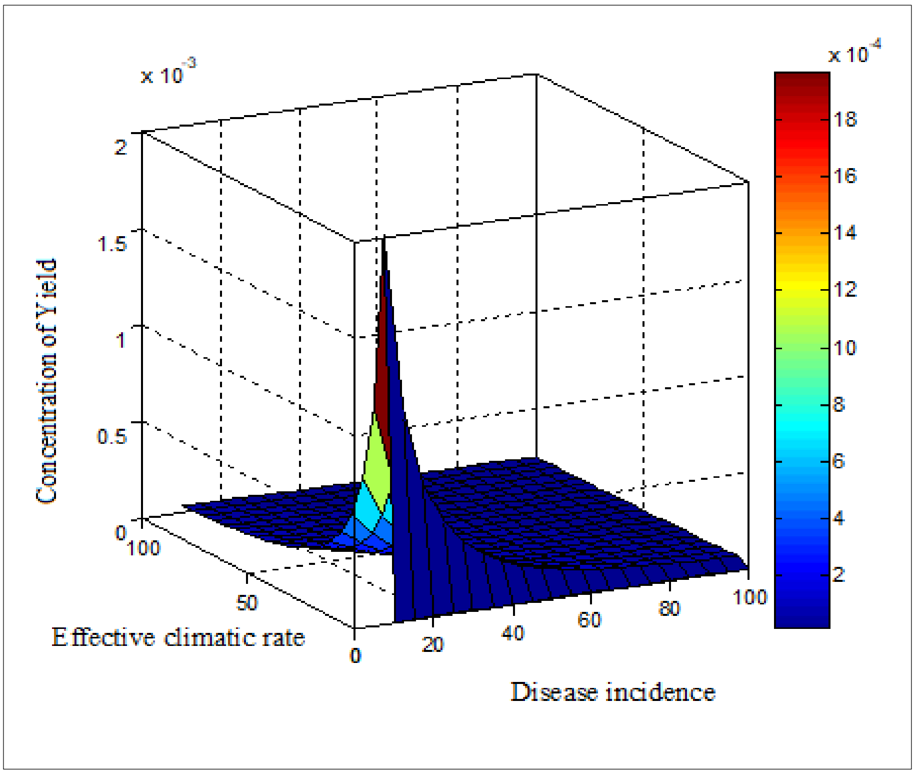

Fig 8: Effects of infection rate α on concentration of yield for varying effective seasonality rate and disease incidence for $C^* = 33, D^* = 0, Y^* = 0, \rho = 0.2.$

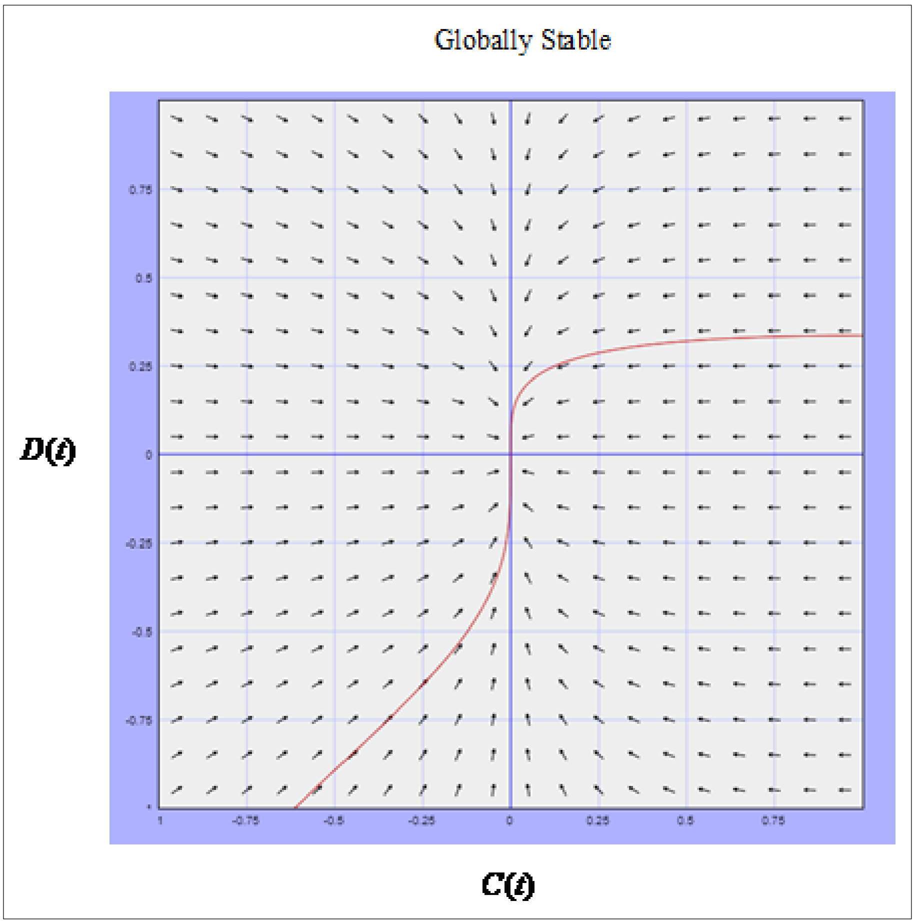

Fig 9: A sketch of the phase plane of the climate disease yield prediction system. Arrows represent the direction of the phase flows of matter through the system.

Table 1: Comparison of analytical result with numerical result for Concentrations $C(t), D(t)$ and $Y(t)$ using the equations (5-7) for experimental values of parameter $C^{*}=33, D^{*}=0, Y^{*}=0, \alpha=23.98, \beta=24.04, \gamma=90, \rho=0.2.$

t	Concentrations								
	$C(t)$			$D(t)$			$Y(t)$		
	This work	**Simulation**	**Error %**	**This work**	**Simulation**	**Error %**	**This work**	**Simulation**	**Error %**
0	28.0000	28.0000	0.0000	0.0000	0.0000	0.0000	0.0000	0.0000	0.0000
0.1	0.00311	0.00312	0.3215	1.6140	1.6150	0.0620	26.3900	26.3800	0.0379
0.2	0.1473	0.1475	0.1358	0.1473	0.1476	0.2037	27.8500	27.8501	0.0004
0.3	0.0120	0.0121	0.8333	0.0121	0.0122	0.8264	27.9900	27.9902	0.0007
0.4	0.0052	0.0052	0.0000	0.00521	0.0052	0.1919	28.0000	28.0000	0.0000
0.5	0.0001	0.0001	0.0000	0.00241	0.00242	0.4149	28.0000	28.0000	0.0000
	Average error %		0.2151	Average error %		0.2832	Average error %		0.0065

Table 2: Monthly meteorological data (2016-20)

Month	Temperature (^{0}C)		Relative Humidity (%)	Rainfall (mm)
	Maximum	**Minimum**		
Feb 2016	31.20	20.64	82.00	-
Mar 2016	35.46	22.19	87.21	2.06
Apr 2016	38.14	25.13	71.44	3.15
May 2016	34.53	25.88	49.00	14.96
Jun 2016	30.20	24.04	73.86	1.58
Jul 2016	30.96	23.81	76.13	2
Aug 2016	31.16	24.91	74.87	1.01
Sep 2016	31.86	23.84	77.13	0.08
Oct 2016	31.36	22.47	75.00	5.23
Nov2016	31.14	21.76	80.10	0.53
Dec 2016	30.65	19.67	86.56	0.69
Jan 2017	30.30	26.80	88.22	43
Feb 2017	32.40	17.60	85.07	1
Mar 2017	32.90	21.40	81.45	77
Apr 2017	36.90	22.40	78.83	44
May 2017	34.80	23.30	74.64	97
Jun 2017	31.20	23.60	73.03	44
Jul 2017	31.70	24.30	69.67	28
Aug 2017	31.60	23.20	68.93	60
Sep 2017	30.70	22.50	68.03	214
Oct 2017	31.40	22.30	71.87	113
Nov2017	30.00	21.20	75.80	233
Dec 2017	28.80	19.60	74.29	64
Jan 2018	30.60	16.80	76.83	2
Feb 2018	32.00	17.30	73.17	21
Mar 2018	33.19	21.32	76.77	22
Apr 2018	35.25	22.58	76.03	25
May 2018	33.19	23.09	79.09	181
Jun 2018	30.60	23.76	78.20	34
Jul 2018	29.22	22.70	76.48	118.5
Aug 2018	29.09	22.93	76.83	131.5
Sep 2018	32.33	22.33	75.23	142
Oct 2018	30.67	21.96	79.22	250
Nov 2018	30.93	22.03	78.63	137
Dec 2018	29.25	20.90	77.97	13
Jan 2019	28.51	16.80	79.70	0.00
Feb 2019	31.74	19.42	71.16	17
Mar 2019	35.14	20.64	76.29	32
Apr 2019	35.33	23.80	78.07	103
May 2019	36.35	26.51	78.96	121
Jun 2019	32.74	23.84	76.13	41
Jul 2019	31.22	22.90	78.41	65
Aug 2019	28.41	22.54	77.58	119
Sep 2019	29.76	22.76	77.00	168

Table 3: Disease intensity of downy mildew for grape during the year 2016-2020 from Theni district

Disease intensity									
	2016-17								
Field no	**1**	**2**	**3**	**4**	**5**	**6**	**7**	**8**	**Avg**
1	3	4	2	2	1	0	1	2	1.88
2	4	0	0	1	0	2	1	1	1.13
3	2	4	3	3	2	1	2	0	2.13
4	3	3	1	2	2	3	1	2	2.13
5	3	3	2	4	3	4	2	3	3.00
6	2	0	3	3	2	2	1	4	2.13
7	1	2	0	3	3	2	3	1	1.88
8	2	4	3	1	3	0	2	2	2.13
9	2	3	3	4	2	2	3	0	2.38
10	1	2	1	2	1	2	3	2	1.75
11	2	3	4	2	2	1	1	1	2.00
12	3	0	1	1	1	1	0	0	0.88
13	2	1	2	1	1	1	2	3	1.63
14	2	1	1	2	1	1	2	2	1.50
15	0	0	1	0	1	1	1	0	0.50
									27.05
	2017-18								
Field no	**1**	**2**	**3**	**4**	**5**	**6**	**7**	**8**	**Avg**
1	2	3	2	2	2	3	1	3	2.25
2	1	1	0	1	0	2	0	1	0.75
3	2	0	1	3	2	1	2	2	1.63
4	1	0	1	0	1	2	1	1	0.88
5	2	1	2	1	2	1	2	2	1.63
6	1	2	3	3	1	2	3	1	2.00
7	1	1	0	3	1	2	3	1	1.50
8	2	1	3	2	2	3	2	3	2.25
9	3	2	0	1	3	2	1	2	1.75
10	3	1	1	1	1	2	3	1	1.63
11	1	3	4	2	1	1	2	3	2.13
12	0	4	1	1	0	1	0	3	1.25
13	2	2	2	1	2	1	1	1	1.50
14	0	1	1	0	0	1	1	1	0.63
15	1	2	1	0	1	1	3	2	1.38
									23.16
	2018-19								
Field no	**1**	**2**	**3**	**4**	**5**	**6**	**7**	**8**	Avg
1	2	2	2	2	1	0	1	2	1.50
2	3	1	0	1	0	2	1	1	1.13
3	2	2	3	3	2	1	2	3	2.25
4	1	0	1	2	1	0	1	1	0.88
5	1	1	2	2	3	2	2	3	2.00
6	1	0	3	3	1	0	1	2	1.38
7	1	1	0	1	1	2	3	1	1.25
8	2	2	3	3	2	3	2	2	2.38
9	2	3	1	0	2	2	1	0	1.38
10	1	2	1	2	1	2	3	2	1.75
11	1	0	0	2	2	1	1	2	1.13
12	3	0	1	0	0	1	1	0	0.75
13	2	1	0	1	1	1	2	2	1.25
14	2	1	2	2	3	3	2	2	2.13
15	0	1	2	2	1	1	3	2	1.50
									22.66
	2019-20								
Field no	**1**	**2**	**3**	**4**	**5**	**6**	**7**	**8**	**Avg**
1	1	3	3	3	2	3	2	2	2.38
2	3	2	2	2	1	2	0	1	1.63
3	0	1	1	0	0	1	1	1	0.63
4	2	3	1	3	2	1	1	4	2.13
5	1	2	2	2	1	2	2	2	1.75
6	1	0	1	0	1	1	1	1	0.75
7	2	1	1	3	1	2	3	12	3.13
8	1	1	1	2	2	1	2	2	1.50
9	1	2	0	1	1	3	1	2	1.38
10	3	1	1	1	1	2	3	2	1.75

11	1	1	1	1	0	0	1	0	0.63
12	0	4	1	1	0	1	0	3	1.25
13	0	2	0	1	2	0	1	1	0.88
14	2	1	1	2	2	4	2	3	2.13
15	1	2	1	0	1	1	3	2	1.38
									23.3

Table 4: Percentage disease incidence of downy mildew for grape during the year 2016-2020 from Theni district

		Raw Data format										
2016-17	**2016-17**	**RI**				**R2**				**R3**		
field no	**Per cent disease incidence**	**No. of grapevine leaves affected**	**Total no. of leaves observed in a set**	**field no**	**Per cent disease incidence**	**No. of grapevine leaves affected**	**Total no. of leaves observed in a set**	**field no**	**Per cent disease incidence**	**No. of grapevine leaves affected**	**Total no. of leaves observed in a set**	**Mean PDI**
1	25.00	3	12	1	40.00	4	10	1	18.18	2	11	27.73
2	18.18	2	11	2	8.33	1	12	2	16.67	2	12	14.39
3	25.00	3	12	3	16.67	2	12	3	25.00	3	12	22.22
4	36.36	4	11	4	27.27	3	11	4	27.27	3	11	30.30
5	36.36	4	11	5	30.00	3	10	5	44.44	4	9	36.94
6	36.36	4	11	6	36.36	4	11	6	41.67	5	12	38.13
7	25.00	3	12	7	45.45	5	11	7	36.36	4	11	35.61
8	36.36	4	11	8	30.00	3	10	8	45.45	5	11	37.27
9	30.77	4	13	9	30.77	4	13	9	20.00	2	10	27.18
10	25.00	3	12	10	36.36	4	11	10	27.27	3	11	29.55
11	15.38	2	13	11	7.69	1	13	11	18.18	2	11	13.75
12	18.18	2	11	12	0.00	0	10	12	8.33	1	12	8.84
13	30.00	3	10	13	27.27	3	11	13	25.00	3	12	27.42
14	16.67	2	12	14	8.33	1	12	14	11.11	1	9	12.04
15	9.09	1	11	15	0.00	0	11	15	12.50	1	8	7.20
												24.57
2017-18		**RI**				**R2**				**RI**		
	Per cent disease incidence	**No. of grapevine leaves affected**	**Total no. of leaves observed in a set**		**Per cent disease incidence**	**No. of grapevine leaves affected**	**Total no. of leaves observed in a set**		**Per cent disease incidence**	**No. of grapevine leaves affected**	**Total no. of leaves observed in a set**	**Mean PDI**
1	33.33	4	12	1	40.00	4	10	1	30.00	3	10	34.44
2	9.09	1	11	2	8.33	1	12	2	16.67	2	12	11.36
3	23.08	3	13	3	41.67	5	12	3	25.00	3	12	29.91
4	8.33	1	12	4	18.18	2	11	4	0.00	0	11	8.84
5	27.27	3	11	5	27.27	3	11	5	23.08	3	13	25.87
6	50.00	5	10	6	33.33	4	12	6	45.45	5	11	42.93
7	8.33	1	12	7	45.45	5	11	7	33.33	4	12	29.04
8	36.36	4	11	8	50.00	5	10	8	41.67	5	12	42.68
9	38.46	5	13	9	38.46	5	13	9	30.00	3	10	35.64
10	25.00	3	12	10	23.08	3	13	10	18.18	2	11	22.09
11	45.45	5	11	11	46.15	6	13	11	33.33	4	12	41.65
12	45.45	5	11	12	16.67	2	12	12	16.67	2	12	26.26
13	30.00	3	10	13	27.27	3	11	13	27.27	3	11	28.18
14	10.00	1	10	14	7.69	1	13	14	7.69	1	13	8.46
15	46.15	6	13	15	36.36	4	11	15	16.67	2	12	33.06
												28.03
2018-19		**RI**				**R2**				**RI**		
	Per cent disease incidence	**No. of grapevine leaves affected**	**Total no. of leaves observed in a set**		**Per cent disease incidence**	**No. of grapevine leaves affected**	**Total no. of leaves observed in a set**		**Per cent disease incidence**	**No. of grapevine leaves affected**	**Total no. of leaves observed in a set**	**Mean PDI**
1	18.18	2	11	1	30.00	3	10	1	27.27	3	11	25.15
2	27.27	3	11	2	8.33	1	12	2	25.00	3	12	20.20
3	30.77	4	13	3	41.67	5	12	3	25.00	3	12	32.48
4	0.00	0	12	4	9.09	1	11	4	11.11	1	9	6.73
5	45.45	5	11	5	36.36	4	11	5	27.27	3	11	36.36
6	30.00	3	10	6	16.67	2	12	6	25.00	3	12	23.89
7	16.67	2	12	7	27.27	3	11	7	18.18	2	11	20.71
8	27.27	3	11	8	40.00	4	10	8	41.67	5	12	36.31
9	23.08	3	13	9	0.00	0	13	9	20.00	2	10	14.36
10	25.00	3	12	10	15.38	2	13	10	18.18	2	11	19.52
11	15.38	2	13	11	15.38	2	13	11	7.69	1	13	12.82
12	9.09	1	11	12	16.67	2	12	12	0.00	0	12	8.59

13	0.00	0	10	13	18.18	2	11	13	23.08	3	13		13.75
14	30.00	3	10	14	30.77	4	13	14	50.00	5	10		36.92
15	30.77	4	13	15	27.27	3	11	15	25.00	3	12		27.68
													22.37
2019-20		**RI**				**R2**				**RI**			
	Per cent disease incidence	**No. of grapevine leaves affected**	**Total no. of leaves observed in a set**		**Per cent disease incidence**	**No. of grapevine leaves affected**	**Total no. of leaves observed in a set**		**Per cent disease incidence**	**No. of grapevine leaves affected**	**Total no. of leaves observed in a set**		**Mean PDI**
1	27.27	3	11	1	30.00	3	10	1	44.44	4	9		33.91
2	30.00	3	10	2	8.33	1	12	2	25.00	3	12		21.11
3	0.00	0	12	3	8.33	1	12	3	8.33	1	12		5.56
4	27.27	3	11	4	40.00	4	10	4	27.27	3	11		31.52
5	36.36	4	11	5	20.00	2	10	5	18.18	2	11		24.85
6	0.00	0	10	6	0.00	0	11	6	30.00	3	10		10.00
7	27.27	3	11	7	40.00	4	10	7	36.36	4	11		34.55
8	16.67	2	12	8	27.27	3	11	8	16.67	2	12		20.20
9	23.08	3	13	9	23.08	3	13	9	20.00	2	10		22.05
10	33.33	3	9	10	30.77	4	13	10	45.45	5	11		36.52
11	0.00	0	12	11	8.33	1	12	11	7.69	1	13		5.34
12	18.18	2	11	12	8.33	1	12	12	16.67	2	12		14.39
13	0.00	0	10	13	18.18	2	11	13	7.69	1	13		8.62
14	30.00	3	10	14	25.00	3	12	14	30.00	3	10		28.33
15	16.67	2	12	15	27.27	3	11	15	8.33	1	12		17.42
													20.96

Table 5: Average value of experimental values of the parameters from Grape research station and surrounding villages at Theni district using the measurement tables (2-4) during the period 2015-2021.

S. No	Parameters	Experimental value (Mean value)
1.	Infection rate (α)	23.98 %
2.	disease incidence (β)	24.04%
3.	seasonality rate (γ)	90%
4.	removal rate of grape yield per harvest time (ρ) (yield loss form GRS)	0.2 to 0.6%
5.	Disease concentration at initial time (D^*)	0
6.	Yield concentration at initial time (Y^*)	0
7.	Climatic concentration at initial time (C^*) (minimum temperature)	33^0c

6. Conclusion

The developed agro-climatic grape yield prediction model (Eq.13) is analytically solved using asymptotic method. The model is quantified in terms of fundamental seasonality index, disease severity rate, infection rate, removal rate of yield loss, the analytical expression of the climate, disease and yield concentration are derived. The obtained results have a good agreement with that numerical result and stability analysis. It is established that the global dynamics are completely determined by the basic reproduction number R_0. If $R_0 \leq 1$, then the disease-free equilibrium is globally asymptotically stable. Therefore, the given system of equation of the model is globally stable. Based on the obtained results of the developed yield prediction model, it is recommended for its use to estimate the grape yield. Also, a valuable tool for predicting crop yields in a few years ahead of time.

Appendix A:

Solution of the equations (5 to7) using Homotopy perturbation method.

In this Appendix, it is indicated how Eqs. (1) to (3) is derived. To find the solution of Eqs. (5) to (7), Homotopy is constructed as follows:

$$(1-p)\left[\frac{dC}{dt}+\gamma C\right]+p\left[\frac{dC}{dt}+\alpha CD+\gamma C\right]=0 \quad \text{(A.1)}$$

$$(1-p)\left[\frac{dD}{dt}+\beta D\right]+p\left[\frac{dD}{dt}+\beta D-\alpha CD\right]=0 \quad \text{(A.2)}$$

$$(1-p)\left[\frac{dY}{dt}+\rho Y\right]+p\left[\frac{dY}{dt}+\rho Y-\beta D-\gamma C\right]=0 \quad (A.3)$$

$$C(0)=C^{*};D(0)=D^{*};Y(0)=Y^{*} \quad (A.4)$$

$$t=0;C_i=0;\mathrm{D}_i=0;\ Y_i=0 \quad (A.5)$$

and

$$\begin{cases} C=C_0+pC_1+p^2C_2+p^3C_3+\ldots\ldots\ldots \\ D=D_0+pD_1+p^2D_2+p^3D_3+\ldots\ldots. \\ Y=Y_0+pY_1+p^2Y_2+p^3Y_3+\ldots\ldots \end{cases} \quad (A.6)$$

Replacing Eq. (A.6) for Eqs. (A.1) and (A.2) and (A.3), the following differential equations areobtained by arranging the power coefficients

$$p^0:\frac{dC_0}{dt}+\gamma C_0=0 \quad (A.7)$$

$$p^1:\frac{dC_1}{dt}+\gamma C_1-\frac{dC_0}{dt}-\gamma C_0+\frac{dC_0}{dt}+\alpha C_0D_0+\gamma C_0=0$$

$$p^1:\frac{dC_1}{dt}+\gamma C_1+\alpha C_0D_0=0 \quad (A.8)$$

$$p^2:\frac{dC_2}{dt}+\gamma C_2-\frac{dC_1}{dt}-\gamma C_1+\frac{dC_1}{dt}+\alpha C_0D_1+\alpha C_1D_0+\gamma C_1=0$$

$$p^2:\frac{dC_2}{dt}+\gamma C_2+\alpha C_0D_1+\alpha C_1D_0=0 \quad (A.9)$$

and

$$p^0:\frac{dD_0}{dt}+\beta D_0=0 \quad (A.10)$$

$$p^1:\frac{dD_1}{dt}+\beta D_1-\alpha C_0D_0=0 \quad (A.11)$$

$$p^2:\frac{dD_2}{dt}-\frac{dD_1}{dt}+\beta D_2-\beta D_1+\frac{dD_1}{dt}+\beta D_1-\alpha C_0D_1-\alpha C_1D_0==0$$

$$p^2:\frac{dD_2}{dt}+\beta D_2-\alpha\left(C_0D_1+C_1D_0\right)=0 \quad (A.12)$$

$$p^0:\frac{dY_0}{dt}+\rho Y_0=0 \quad (A.13)$$

$$p^1:\frac{dY_1}{dt}+\rho Y_1-\gamma C_0-\beta D_0=0 \quad (A.14)$$

Using the above equation, the following results are found.

$$C_0 = C^* e^{-\gamma t} \tag{A.15}$$

$$D_0 = D^* e^{-\beta t} \tag{A.16}$$

$$Y_0 = Y^* e^{-\rho t} \tag{A.17}$$

$$C_1 = -\frac{\alpha C^* D^*}{\beta} e^{-\gamma t} + \frac{\alpha C^* D^*}{\beta} e^{-(\beta+\gamma)t} \tag{A.18}$$

$$D_1 = \frac{\alpha C^* D^*}{\gamma} e^{-\beta t} - \frac{\alpha C^* D^*}{\gamma} e^{-(\beta+\gamma)t} \tag{A.19}$$

$$Y_1 = \left(\frac{\gamma C^*}{\gamma - \rho} + \frac{\beta D^*}{\beta - \rho}\right) e^{-\rho t} + \frac{\gamma C^*}{\rho - \gamma} e^{-\gamma t} + \frac{\beta D^*}{\rho - \beta} e^{-\beta t} \tag{A.20}$$

$$C_2 = \left(\frac{\alpha^2 C^{*2} D^*}{\beta\gamma} - \frac{\alpha^2 C^{*2} D^*}{(\beta+\gamma)} - \frac{\alpha^2 C^* D^{*2}}{2\beta^2}\right) e^{-\gamma t} - \frac{\alpha^2 C^{*2} D^*}{\beta\gamma} e^{-(\beta+\gamma)t} + \frac{\alpha^2 C^{*2} D^*}{(\beta+\gamma)} e^{-(\beta+2\gamma)t}$$
$$+ \frac{\alpha^2 C^* D^{*2}}{\beta^2} e^{-(\beta+\gamma)t} - \frac{\alpha^2 C^* D^{*2}}{2\beta^2} e^{-(2\beta+\gamma)t} \tag{A.21}$$

$$D_2 = \left(\frac{\alpha^2 C^{*2} D^*}{2\gamma^2} - \frac{\alpha^2 C^* D^{*2}}{\gamma\beta} + \frac{\alpha^2 C^* D^{*2}}{(\beta+\gamma)}\right) e^{-\beta t}$$
$$- \frac{\alpha^2 C^{*2} D^*}{\gamma^2} e^{-(\beta+\gamma)t} + \frac{\alpha^2 C^{*2} D^*}{2\gamma^2} e^{-(\beta+2\gamma)t} + \frac{\alpha^2 C^* D^{*2}}{\gamma\beta} e^{-(\beta+\gamma)t} - \frac{\alpha^2 C^* D^{*2}}{(\beta+\gamma)} e^{-(2\beta+\gamma)t} \tag{A.22}$$

According to the HPM, it can be concluded that

$$C(\rho) = \lim_{p\to 1} C(\rho) = C_0 + C_1 + \ldots\ldots\ldots\ldots\ldots\ldots \tag{A.23}$$

$$D(\rho) = \lim_{p\to 1} D(\rho) = D_0 + D_1 + \ldots\ldots\ldots\ldots\ldots\ldots \tag{A.24}$$

$$Y(\rho) = \lim_{p\to 1} Y(\rho) = Y_0 + Y_1 + \ldots\ldots\ldots\ldots\ldots\ldots\ldots\ldots \tag{A.25}$$

After putting Eqs. (A.15), (A.18) and (A.21) into Eq. (A.23), Eqs.(A.16), (A.19) and (A.22) into Eq. (A.24) and Eqs. (A.17) and (A.20) into Eq.(A.25), the final results can be described in Eqs. (3) to (6) in the text. The remaining components of $C_n(x), D_n(x)$ and $Y_n(x)$ are entirely defined in such a way that the previous term decides each term.

Appendix B

Matlab Program for the Numerical Solution of Nonlinear Differential Eqs. (13-15)

function main options= odeset ('RelTol',1e-6,'Stats','on');% initial conditions C=33; D=0.0001; Y=0; Xo = C, D, Y]; tspan = [0,0.5]; xspan = [0,100]; tic [t,X] = ode45(@TestFunction,tspan,Xo,options); toc figure plot(t,X(:,1),t,X(:,2),t,X(:,3)) ylabel('x') xlabel('t') return function [dx_dt]= Test Function (t, x) a=23.98; b=24.04; r=90; dx_dt(1) =-a*x(1)*x(2)-r*x(1); dx_dt(2) =a*x(1)*x(2)-b*x(2); dx_dt(3) =b*x(2)+r*x(1); dx_dt = dx_dt'; return.

Acknowledgement

This work is supported by Science and Engineering Research Board under MATRICS (SERB - No.: MTR/2019/001221). The Authors are very grateful to the reviewers for their careful and meticulous reading of the paper. They also express their gratitude to Dr. V. Geethalakshmi, Vice Chancellor, Dr. M. Raveendran, Director of Research, Tamil Nadu Agricultural University, Coimbatore, Professor& Head, Dept. of PS&IT, Agricultural Engineering College and Research Institute, TNAU, Coimbatore.

7. References

1. Emmett RW, *et al*. Grape diseases and vineyard protection, In B.G. Coombe & P.R. Dry (ed) Viticulture 1992;2:232-278.
2. Magarey PA, *et al*. A computer based simulator for rational grapevine downy mildew (*plasmopara viticola*) on grape leaves. Phytopathology. 1994;78:1316-1321.
3. Blaise P, Gessler C. Development of a forecast model of grape downy mildew on a microcomputer in II International Symposium on Computer Modelling. Fruit Research and Orchard Management. 1990;276:63-70.
4. Hill GK. Plasmopara Risk Oppenheim–a deterministic computer model for the viticultural extension service. Notsulle Mal. dellePiante. 1990;111:231-238
5. Magarey PA, Wachtel MF, Weir PC, Seem RC. A computer based simulator for rational management of grapevine downy mildew (*Plasmopara viticola*). Plant Prot. 1991;6:29-33.
6. Magnien C, Jacquin D, Muckensturm N, Guillemard P. MILVIT: a descriptive quantitative model for the asexual phase of grapevine downy mildew. IOBC/WPRS Buletin. 1991;21:451-459.
7. Orlandini S, Gozzini B, Rosa M, Egger E, Storchi P, Maracchi G, *et al*. PLASMO: a simulation model for control of *Plasmopara viticola* on grapevine. EPPO Bull. 1993;23:619-626.
8. Ellis MA, Madden LV, Lalancette N. A disease forecasting program for grape downy mildew in Ohio. Special report (New York State Agricultural Experiment Station; USA). 1994;68:92-95.
9. Blaise PH, Dietrich R, Gessler C. Vinemild: an application oriented model of *Plasmopara viticola* epidemics on *Vitis vinifera*. In V International Symposium on Computer Modelling in Fruit Research and Orchard Management. 1999;499:187-192.
10. Leroy P, Smits N, Cartolaro P, Deliere L, Goutouly JP, Raynal M, *et al*. A bioeconomic model of downy mildew damage on grapevine for evaluation of control strategies. Crop Prot. 2013;53:58-71.
11. Christopher A Gilligan, Simon gubbins, Sarah A Simons. Analysis and fitting of an SIR model with host response to infection load for a plant disease. Phil. Trans. R. Soc. Lond. B. 1997;352:353-364.
12. Daniele Bevacqua, Benedicte Quilot-Turion, Luca-Bolzoni. A Model for temporal dynamics of brown rot spreading in fruit orchards. Phytopathology. 2018;108:595-601.
13. Jeger MJ, Jeffries P, Elad Y, Xu XM. A generic theoretical model for biological control of foliar plant diseases. Journal of Theoretical Biology. 2009;256:201-214.
14. Nurul S, Abdul Latif, Graeme C Wake, Tony Reglinski, Philip AG, Elmer, Joseph T Taylor, *et al* Modelling the induced resistance to plant disease using a dynamical system approach. Frontiers in plant science. 2014;4:1-53.
15. Mario De La Fuente, Ruben Linares, Pilar Baeza, Carlos Miranda, Jose Ramon Lissarrague. Comparison of different methods of grapevine yield prediction in the time window between fruitset and veraison. J Int. Sci. Vigne Vin. 2015;49:27-35.
16. Rory Ellis, Elena Moltchanova, Daniel Gerhard, Mike Trought, LinLin Yang. Using Bayesian growth models to predict grape yield. OENO One. 2020;54(2):443-453.
17. Vittorio Rossi, Tito Caffia, Simona Giosue, Riccardo Bugiani. A mechanistic model simulating primary infections of downy mildew in grapevine. Ecological modelling. 2008;212:480-491.
18. Nurul S, Abdul Latif, Graeme C Wake, Tony Reglinski, Philip AG, Elmer. Modelling induced resistance to plant diseases. Journal of Theoretical Biology. 2014;47:144-150.
19. Manisha S Sirsata, Jonao Mendes-Moreiraa, Carlos Ferreiraa, Mario Cunha. Machine Learning Predictive Model of Grapevine Yield based on Agroclimatic Patterns. Environment and food, 2019.
20. Estefania Gonzalez Fernandez, Alba Pina-Rey, MariaFernandez-Gonzalez, Maria J Aira, Javier F. Rodriguez-Rajo. Prediction of Grapevine Yield Based on Reproductive Variables and the Influence of Meteorological Conditions, Agronomy. 2020;10:714.
21. Kadbhane SJ, Manekar VL. Development of agro-climatic grape yield model with future prospective, Italian Journal of Agrometeorology. 2021;1:89-103.